minerals

MDPI

Article

Novel Selective Depressant of Titanaugite and Implication for Ilmenite Flotation

Nengyun Liu [1,2], Zhen Wang [3,*], Junhui Xiao [3,*], Hongbin Wang [1], Bing Deng [1,2], Yushu Zhang [2] and Chao Chen [2]

1 State Key Laboratory of Vanadium and Titanium Resources Comprehensive Utilization, Panzhihua 617000, China; liunengyuncsu@163.com (N.L.); wanghongbin@ansteel.com.cn (H.W.); dbing86@163.com (B.D.)
2 Institute of Multipurpose Utilization of Mineral Resources, Chinese Academy of Geological Sciences, Chengdu 610041, China; zys2621@126.com (Y.Z.); chenchao43420@126.com (C.C.)
3 School of Environment and Resource, Southwest University of Science and Technology, Mianyang 621010, China
* Correspondence: wangzhen@swust.edu.cn (Z.W.); xiaojunhui@swust.edu.cn (J.X.)

Received: 26 September 2019; Accepted: 11 November 2019; Published: 13 November 2019

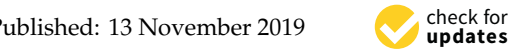

Abstract: This paper studies the effects of sodium polystyrene sulfonate (PSSNa) used as a depressant upon the separation of ilmenite from titanaugite through flotation when sodium oleate (NaOl) is used as a collector by performing single mineral flotation experiments. The depression mechanism of PSSNa on titanaugite flotation was studied by electrokinetic potential and adsorbed amount measurements together with FTIR and XPS detection. Single mineral flotation experiments show that PSSNa is a selective depressant for the separation of ilmenite and titanaugite via flotation with NaOl as the collector. The results of the adsorbed amount tests show that the biggest distinction is in terms of the amount of NaOl adsorbed on the surfaces of ilmenite and titanaugite; the amount is expanded from 2.28×10^{-7} to 9.34×10^{-7} mol/m^2 when the dosage of PSSNa is 1 mg/L, as compared with no PSSNa, suggesting that PSSNa is a selective depressant when separating ilmenite and titanaugite through flotation. FTIR testing shows that chemisorption has occurred between the $-SO_3^-$ groups of the molecular PSSNa and titanaugite surfaces. The results of further XPS testing reveal that PSSNa chemically interacts with Ca/Mg/Al/Fe on the titanaugite surface. The test results of FTIR in combination with XPS confirm that PSSNa stops NaOl from interacting with Mg, Fe, Al, and Ca on the titanaugite surface, and this outcome is the main reason for the widening of the adsorption quantity gap of NaOl on titanaugite and ilmenite surfaces, and titanaugite flotation is suppressed. The results of the comparison flotation testing on actual Panzhihua titanic iron ore (TiO_2 grade: 15.63%) with titanaugite as the main gangue show that a better effect is obtained by replacing sodium silicate (SS) with PSSNa, and the recovery of TiO_2 using PSSNa is higher than that when using sodium silicate. In a closed circuit flotation test, ilmenite concentrate is obtained with a TiO_2 grade of 45.97% and a recovery of 76.32% by using PSSNa as a titanaugite depressant.

Keywords: sodium polystyrene sulfonate; depressant; titanaugite; selective flotation; adsorption

1. Introduction

Titanium is lightweight, highly resistant to corrosion and high-strength metal. Considering the stable chemical properties, as well as the favorable high-temperature, low-temperature, and strong acid and alkali resistance characteristics, Ti has been utilized in broad applications in many aspects such as the military industry, aerospace, environmental protection, transportation, and medical device manufacturing [1,2]. Ilmenite, anatase, perovskite, brookite, and rutile are among the chief resources of Ti showing industrial application significance. Among these minerals, rutile and ilmenite have

experienced great development and utilization [3,4]. Currently, as natural rutile becomes less abundant, ilmenite is becoming the most important titanium resource [2,5]. Ilmenite is shown as (Fe, Mg, Mn)TiO_3 with regard to the detailed formula, in which Mg and Mn of limited quantities displace Fe or Ti at primary ilmenite lattices [6]. Titanic iron ores are conventionally beneficiated by use of methods such as separation based on magnetism, gravity, and electrostatic properties or by combining the above technologies [7]. However, the above methods are not that efficient when fine-sized ilmenites spread in gangue. As a physicochemical method, froth flotation is effective in selectively separating ilmenite from diverse ores [4,8,9]. Nevertheless, titanaugite has similar physiochemical properties as ilmenite. The metal ions on their surfaces consist of Fe^{3+}, Fe^{2+}, Ca^{2+}, Mg^{2+}, and Al^{3+}, and the relationship of pH with the standard Gibbs free energy (ΔG^{θ}) of these metallic ions reacting with oleate can be calculated by the solubility product of oleate and constants for the accumulation stability of the hydroxo complex of metallic ions [10]. According to the results within the weak acid pH range from 5 to 6, the ΔG^{θ} values of all of these metallic ions are negative values, and the e and titanaugite laccalculation results indicated that interactions between fatty acids and metallic ions on the surfaces of ilmenitk selectivity. The findings of Fan [4] also confirm that it is difficult to selectively separate ilmenite from titanaugite through froth flotation based on the interaction of a fatty acid collector with the titanaugite surface through chemisorption under the condition of absence of depressants. Therefore, depressants must be used in the ilmenite flotation process to improve the selectivity of flotation separation. Sulfuric acid, sodium silicate, oxalic acid and acid water glass are conventional depressants of titanaugite during flotation. Sulfuric acid depresses the floatability of titanaugite by means of dissolution of Mg^{2+} and Ca^{2+} on the surface of titanaugite interacting with sodium oleate (NaOl) [11]. Studies have shown that the acidized water glass produced negatively charged colloidal silica, which was adsorbed selectively on the surfaces of gangue minerals during the flotation process of ilmenite [9,12]. Oxalic acid exerts an inhibitory effect on the floatability of titanaugite because calcium oxalate precipitation forms on the titanaugite surface [13]. The floatability of titanaugite is depressed during flotation, mainly by two methods, including calcium and magnesium ion dissolution on the titanaugite surface and chemical interaction between depressants and calcium and magnesium ions on the titanaugite surface. The present research about titanaugite depressant is mainly water glass or oxalic acid [12,13]. The study of high molecular weight organic compounds used as titanaugite depressants is less common; polymeric PSSNa was used as titanaugite depressant in this article, and the depressant mechanism of a PSSNa polymer during the floatation of titanaugite was studied.

2. Materials and Methods

2.1. Mineral Samples

Raw ores for preparing pure minerals were obtained from tailings of magnetic separation in a titanium processing plant (Lomon Corporation, Panzhihua, China). Pure minerals of ilmenite together with titanaugite were obtained from the raw ore by magnetism and gravity. Pure minerals were dry milled by using a jar mill, and the −0.074+0.038 mm fractions of pure minerals were used for the flotation and adsorption tests, and −0.038 mm fraction test experiments. Sulfuric acid, sodium hydrate, NaOl and PSSNa were analytical reagent grade. The molecular structure of PSSNa is shown in Figure 1. The XRD results of pure ilmenite and titanaugite minerals obtained using the Jade 6.0 Package are shown in Figure 2, and both minerals' purity levels are more than 96% through comparison with the corresponding PDF cards in Jade (version 6.0, Materials Data, Inc., Leominster, MA, USA). The specific surface areas of these two pure mineral samples (−0.074 and +0.038 mm) were tested by the method of N_2 adsorption analysis using a Micromeritics ASAP 2010 detection device (Micromeritics Instrument corporation, Norcross, GA, USA) and shown in Table 1. Table 1 lists the results of the chemical composition analysis and specific surface area of two pure minerals, which revealed that ilmenite and titanaugite have purities higher than 95%.

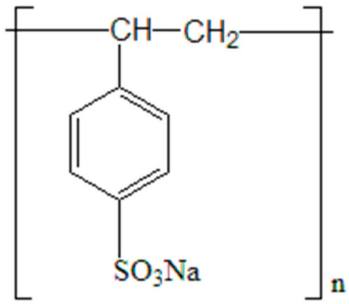

Figure 1. The molecular structure of PSSNa.

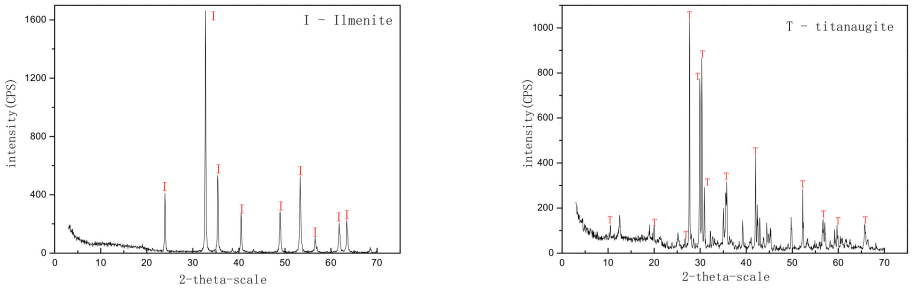

Figure 2. XRD graphics of purified titanaugite and ilmenite.

Table 1. Chemical compositions and specific surface areas of the samples after being purified (mass fraction %).

Samples	TiO_2	Fe_2O_3	MgO	Al_2O_3	SiO_2	CaO	MnO	Specific Surface Area/$m^2 \cdot g^{-1}$
Ilmenite	51.14	39.21	4.46	1.85	1.47	0.37	0.61	0.89
Titanaugite	1.91	14.58	11.36	5.88	41.09	18.16	0.17	0.74

2.2. Flotation

2.2.1. Microflotation

Floatability tests were conducted in a 40 mL micro-flotation cell. Pure mineral particles (2.0 g) were placed in plexiglass cells for 2 min to be conditioned, and then, pH regulators, i.e., HCl or NaOH, were added for adjustment to the needed pH. Under this desired pH, PSSNa depressant was added, followed by NaOl collector, with 3 min of stirring after each addition. After all of the above was finished, the flotation process was performed for 4 min. After being filtered and dried, the froth products together with the tails were separately weighed. Then, the recovery was solved in accordance with the dry weight of products. The researchers established three flotation tests in the same conditions to report average values of the three methods.

2.2.2. Bench Scale Flotation

The raw ore for flotation testing is the strongly magnetic coarse concentrate obtained from the tailings of Panzhihua ore dressing plant (Lomon Corporation, Panzhihua, China), and the magnetic coarse concentrate content passing 74 μm is 73%. Table 2 depicts the results of the XRF analysis of the flotation raw ores and shows that the TiO_2 grade is 15.63%. The closed-circuit flow sheet with one roughing, one scavenging and four cleanings is shown in Figure 3. Two hundred and fifty grams of raw ore for flotation was placed into the 0.75 L flotation cell (XFD-type flotation apparatus, Jilin Exploration Machinery Plant, Changchun, China), and the flotation cell was filled with water to prepare a pulp with the solid concentration of approximately 30 wt %. H_2SO_4 (4000 g/t) was added into the slurry, at

which point the pH value of slurry was approximately 5–6, and then, depressant PSSNa (250 g/t) or sodium silicate (SS, 250 g/t) was immediately added. The slurry was conditioned for 3 min, and after completing the above steps, the collector CT (4000 g/t, fatty acid-based organic mixture) was added into the slurry; the slurry was conditioned for 5 min. The flotation process was started to obtain foam products of roughing titanium concentrate after the slurry conditioning process was completed; then the remaining pulp in the flotation cell were conditioned again with H_2SO_4 (1000 g/t, PSSNa (65 g/t) or sodium silicate (65 g/) and collector CT(500 g/t). Other foam products were collected as scavenging titanium concentrate, and the remaining pulp in the flotation cell was eventually flotation tailings. The foam products from roughing (roughing ilmenite concentrate) were transferred into a 0.5 L flotation cell (XFD-type flotation apparatus); H_2SO_4 (2000 g/t), PSSNa (150 g/t) were added in turn and the pulp is stirred 3 min, then the foam products were collected to complete the first cleaning; the remaining pulp in the flotation cell and scavenging concentrate were returned to the roughing; the foam products from the first cleaning were transferred to 0.5 L flotation cell (XFD-type flotation apparatus), changing the dosage of H_2SO_4 and PSSNa (see Figure 3) and operating three times according to the same method during the second cleaning to forth cleaning; the foam products from the fourth were final ilmenite concentrate, and the remaining pulp in the flotation cell during each cleaning was returned to the previous cleaning operation. The final titanium concentrate was collected after four cycles of cleaning flotation from roughing titanium concentrate. The final titanium concentrate and eventual flotation tailings were filtered, dried, weighed and analyzed for TiO_2.

Table 2. XRF results of actual raw ore.

Component	Fe	TiO_2	S	P_2O_5	Na_2O	K_2O	CaO	Al_2O_3	MgO	SiO_2
Content (%)	16.628	15.617	0.08	0.122	0.747	0.307	11.251	6.101	8.915	30.843

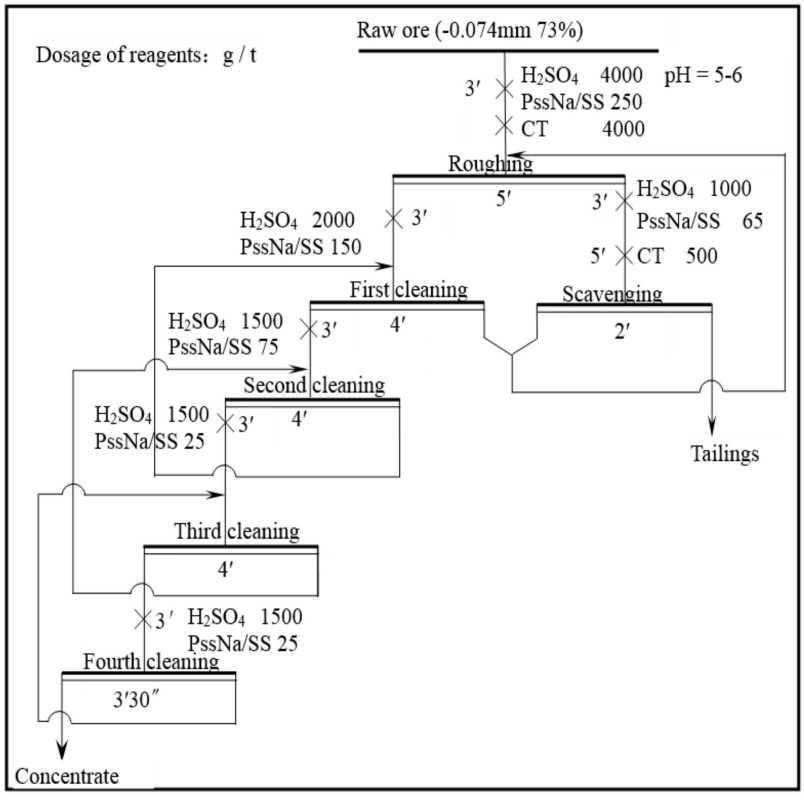

Figure 3. Flow chart of closed circuit flotation test (′ is for minute and ″ is for second).

2.3. Electrokinetic Potential Tests

By employing a zeta potential analyzer (ZetaPlus, Bruker, Germany), the electrokinetic potential values were measured at 20 ± 0.5 °C. Then, at a given pH and reagent concentration, a preparation of mineral (−5 μm) solutions containing solids (0.02 g) and KCl (40 mL, 1 mM) background electrolyte was carried out in a beaker. After letting the solutions stand for 5 min, the supernatants were taken and adopted to measure the electrokinetic potential. For the mineral/depressant/collector system, the sample was successively conditioned with depressant and collector solution.

2.4. Adsorption Measurements

By measuring absorbance at two wavelengths (225 and 233 nm) for PSSNa and NaOl utilizing an ultraviolet (UV-3100) spectrometer (Shimadu Corporation, Kyoto, Japan) [14,15], respectively; the amounts absorbed onto the minerals were determined in the pH range of 6 ± 0.5. After pulping a 2.0 g sample with 40 mL of distilled water, the researchers stirred the solution for 15 min with the addition of given amounts of desired reagents and then used a high speed refrigerated centrifuge (Hitachi Corporation, Tokyo, Japan) to centrifuge the solution for 10 min at 4500 rpm. Then, the residual concentration of reagents in supernatant was detected using the UV spectrometer. The quantities of the reagents adsorbed on the minerals were computed according to differences in the initial and residual concentrations of the reagents. As for the adsorption of NaOl with the PSSNa tests, each sample was conditioned 3 min with desired PSSNa and then 1×10^{-4} M NaOl was added into the collector solution.

2.5. FTIR Measurement

A Fourier transform infrared (FTIR) (USA) spectrometer (Version BM) (PerkinElmer Corporation, Waltham, MA, USA) was utilized to record the FTIR spectra at 25 °C between 4000 and 450 cm^{-1}. KBr pellets were adopted to measure the spectra of the solids. Pure minerals for tests were ground into particles of less than 5 μm. Two grams of purified mineral at less than 5 μm and reagents for flotation were placed in a blending cell for 40 min with reagents, as in the above microflotation test procedures without a NaOl collector. Then, ultrapure water was used to wash the solid samples three times, which were then dried at temperatures below 50 °C for the FTIR tests. These procedures have been used in numerous relevant studies [16,17].

2.6. XPS Measurements

An XSAM800 spectrometer (Kratos, Manchester, UK) was used for the determination of the XPS spectra of the titanaugite and ilmenite powders. The pressure in the analysis chamber was less than 2×10^{-7} mbar. Al Kα X-rays with 1486.6 eV of energy and 12 kV × 15 mA of power for narrow scans were employed for observations. The treated and untreated −5 um minerals were dried in a vacuum oven at 40 °C and subsequently tested by the meter at ambient temperature. The C 1s peak was referenced to a binding energy (BE) for uncharged hydrocarbons at 284.8 eV [18]; the detection process was carried out in FAT mode, and the spectrometer was calibrated with $Cu_{2p3/2}$/(932.67 eV), Ag_3d_5/(368.30 eV), and $Au_4f_{7/2}$/(84.00 eV) standard samples. XPS Peak Fit software (version 4.1) was used for data fitting.

3. Results and Discussion

3.1. Flotation

3.1.1. Microflotation

Flotation tests of single minerals were performed to explore the effects of PSSNa dosage and pH upon the recovery of ilmenite and titanaugite, with the results demonstrated in Figure 4. As illustrated in Figure 4A, ilmenite has good floatability in the pH range of 4–10, while titanaugite is floatable in neutral and strongly alkaline conditions, conforming to previous findings [11,19]. The pH range of

3–4, in which the difference in recoveries of the two minerals is greater, is too narrow to easily control effective separation, and this pH range is not suitable for practical application. Figure 4A also indicates that PSSNa distinctly inhibits the floatability of titanaugite, while this depressive effect is negligible for ilmenite, resulting in a broader pH range of 3–10 for effective separation of ilmenite from titanaugite. With continued observation of the difference in the recovery of minerals with and without PSSNa, this difference is greatest at approximately pH 6. The effect of PSSNa concentration on mineral flotation with NaOl as a collector at a pH of 6 was thus investigated, with the results shown in Figure 4B. With the increasing PSSNa concentration, the recovery of titanaugite via flotation decreases rapidly; that of ilmenite, however, decreases slightly. When adding 1 mg/L of PSSNa, 60% and 5% of ilmenite and titanaugite were recovered, respectively. PSSNa behaved as a selective depressant for ilmenite and titanaugite flotation separation.

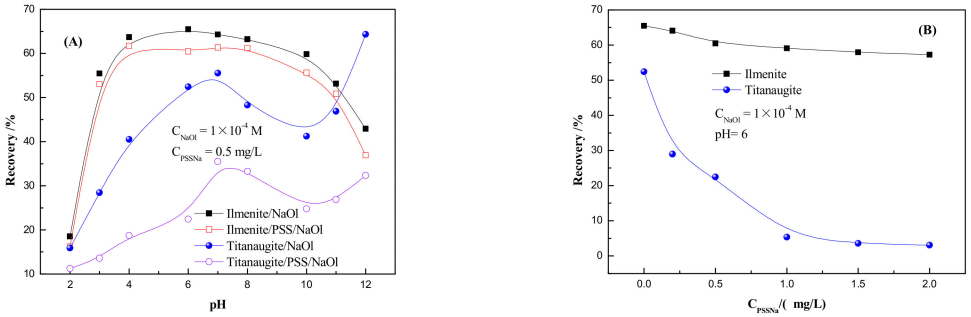

Figure 4. Effects of pH (**A**) and PSSNa concentration (**B**) on recovery of ilmenite and titanaugite.

3.1.2. Bench Scale Flotation

As shown in the figure and by the results in Table 3, with PSSNa as the depressant, the optimal TiO_2 grade of ilmenite concentrate is 45.97%, with a recovery of 76.32%, while with conventional SS as the depressant, optimal TiO_2 grade of the ilmenite concentrate is 43.54% with a recovery of 70.18%. 6% recovery increase was achieved by the replacement of SS with PSSNa, and the grade surpassed the lowest standard of Ti concentrate (44%) in China. Moreover, the TiO_2 grade in the tailings with PSSNa as a depressant was lower than that with SS, showing that the novel selective depressant PSSNa is superior to conventional SS for this sample. The XRD patterns of concentrate and tailings are show in Figure 5a,b, respectively. It can be found that the ilmenite and taitanaugite are relatively concentrated in concentrate and tailings, respectively, presenting good consistence with the results from chemical analysis in Table 3.

Table 3. Results of closed circuit flotation test.

Product Name	Yield (%)		TiO_2 Grade (%)		TiO_2 Recovery (%)	
	PSSNa	Sodium Silicate	PSSNa	Sodium Silicate	PSSNa	Sodium Silicate
Ilmenite concentrate	25.93	25.19	45.97	43.54	76.32	70.18
Tailings	74.07	74.81	5.01	6.23	23.68	29.82
Crudes	100.00	100.00	15.63	15.63	100.00	100.00

Optimal PSSNa and SS dosages were used.

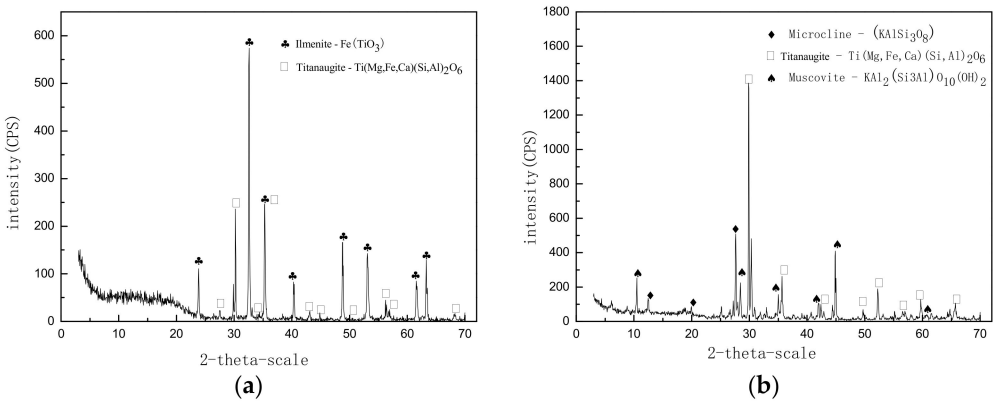

Figure 5. XRD patterns of (**a**) the concentrate and (**b**) the tailings of the raw ore flotation.

3.2. Electrokinetic Potential

To understand the selective depression mechanism of PSSNa for the ilmenite/titanaugite system, electrokinetic potentials of the two minerals are detected in conditions with and without reagents. After testing, the isoelectric points of the raw titanaugite and ilmenite are 3.8 and 5.9, respectively, being in the range of previous reports [7,20], as shown in Figure 6.

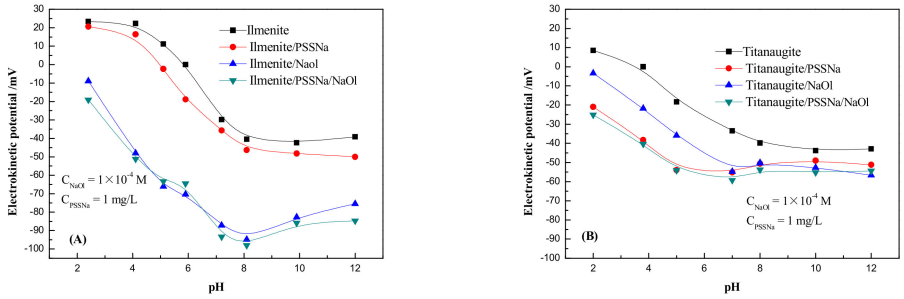

Figure 6. Zeta potential values shown as a function of pH for (**A**) ilmenite and (**B**) titanaugite before and after interaction with reagents.

From Figure 6A,B, the variation in the electrokinetic potential of titanaugite is much greater than that of ilmenite before and after interaction with PSSNa, indicating a stronger adsorption of PSSNa on the titanaugite surface. In the same way, the stronger adsorption of NaOl on ilmenite versus that on titanaugite can be concluded. The adsorption of negatively charged PSS- and Ol-causes the decrease in electrokinetic potential. This outcome agrees with the test results of microflotation. According to the comparative observation of the curves for ilmenite/PSSNa and ilmenite/PSSNa/NaOl in Figure 6A, the large change in electrokinetic potential reflects the fact that the PSSNa pretreated ilmenite can still adsorb NaOl strongly, while by contrasting the curves for titanaugite/PSSNa and titanaugite/PSSNa/NaOl in Figure 6B, no obvious variation is observed, indicating that little NaOl can be adsorbed onto the PSSNa pretreated titanaugite surface.

3.3. Adsorption Amounts

To quantitatively clarify the adsorption of PSSNa on titanaugite and ilmenite and determine its effect on NaOl adsorption, adsorption tests were carried out, and the amounts of NaOl and PSSNa adsorbed onto the surfaces of titanaugite and ilmenite were taken as functions of concentration of PSSNa (C_{PSSNa}) and pH (Figure 7). With increasing pH, the adsorbed amount of PSSNa on titanaugite reached its maximum at pH 6, showing good agreement with flotation results. With no PSSNa in the mineral slurry, the adsorbed amounts of NaOl onto ilmenite and titanaugite are 10.84×10^{-7} and 8.56×10^{-7} mol/m^2, respectively. Once the depressant PSSNa was added, the amounts of NaOl

adsorbed onto the surfaces of the two minerals declined within the experimental range of concentration at a pH value of 6.0, while the descending amplitude for titanaugite was much greater than that for ilmenite. With 1 mg/L C_{PSSNa}, the amounts of NaOl that were adsorbed onto the surfaces of ilmenite and titanaugite declined by 10% and 94%, respectively. Pre-adsorbed PSSNa more strongly inhibits the adsorption of NaOl onto titanaugite than onto ilmenite.

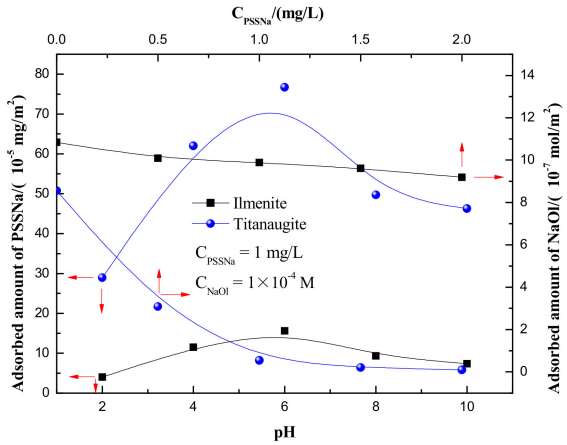

Figure 7. Adsorbed amount of PSSNa onto ilmenite and titanaugite as a function of pH with a PSSNa initial concentration of 1 mg/L and that of NaOl onto the ilmenite and titanaugite treated with PSSNa versus C_{PSSNa} with NaOl initial concentration of 1×10^{-4} M at pH 6.0.

3.4. FTIR

FTIR spectra for titanaugite/ilmenite, NaOl and PSSNa, as well as titanaugite/ilmenite treated with PSSNa or NaOl, are shown in Figure 8a–c. It can be seen from the spectra of PSSNa that the signal of the hydroxyl peak in the sulfonate group opposite PSSNa emerges at 3425 cm^{-1} [21], the vibration peak of methylene $–CH_2$ on the benzene ring appeared at 2923 cm^{-1} [22], the peak for the stretching vibration of –C=C– appeared at 1636 cm^{-1} [23], and the peaks of stretching vibrations of O=S=O in $–SO_3H$ appeared at 1184 and 1129 cm^{-1} [24–28]. The bands at approximately 1402 and 1020 cm^{-1} were attributed to vibrations of benzene rings of PSSNa [29–31]. From Figure 8c, the FTIR spectra of titanaugite treated with PSSNa exhibit a number of newly appearing strong peaks. Newly appearing peaks at 1169, 956, and 2923 cm^{-1} are attributed to the O=S=O, benzene ring group and $–CH_2$ stretching vibrations in the PSSNa molecule, the peaks for O=S=O and benzene ring shift by 15 and 64 cm^{-1}, respectively, and new peaks appear (597, 518, and 473 cm^{-1}). Compared with the FTIR spectra of pure titanaugite, we can deduce that different vibration absorption peaks located at 1169, 956, 597, 518, and 473 cm^{-1} appeared on the titanaugite surface. It can thus be inferred that PSSNa molecules interact with metal ions on the titanaugite surface and adsorb onto the titanaugite surface. As shown in Figure 8b,c, weak characteristic peaks corresponding to O=S=O and –C=C– can be found and illustrate a stronger interaction between PSSNa and titanaugite than that between PSSNa and ilmenite. The results of FTIR detection show good agreement with electrokinetic potential and adsorption tests. Without PSSNa, NaOl can adsorb on both mineral surfaces. For mineral surface treated with PSSNa, the adsorption of NaOl on titanaugite is inhibited while that on ilmenite is almost not affected, reflected by the similar spectra for titanaugite/PSSNa with titanaugite/PSSNa/NaOl and ilmenite/NaOl with ilmenite/PSSNa/NaOl, respectively.

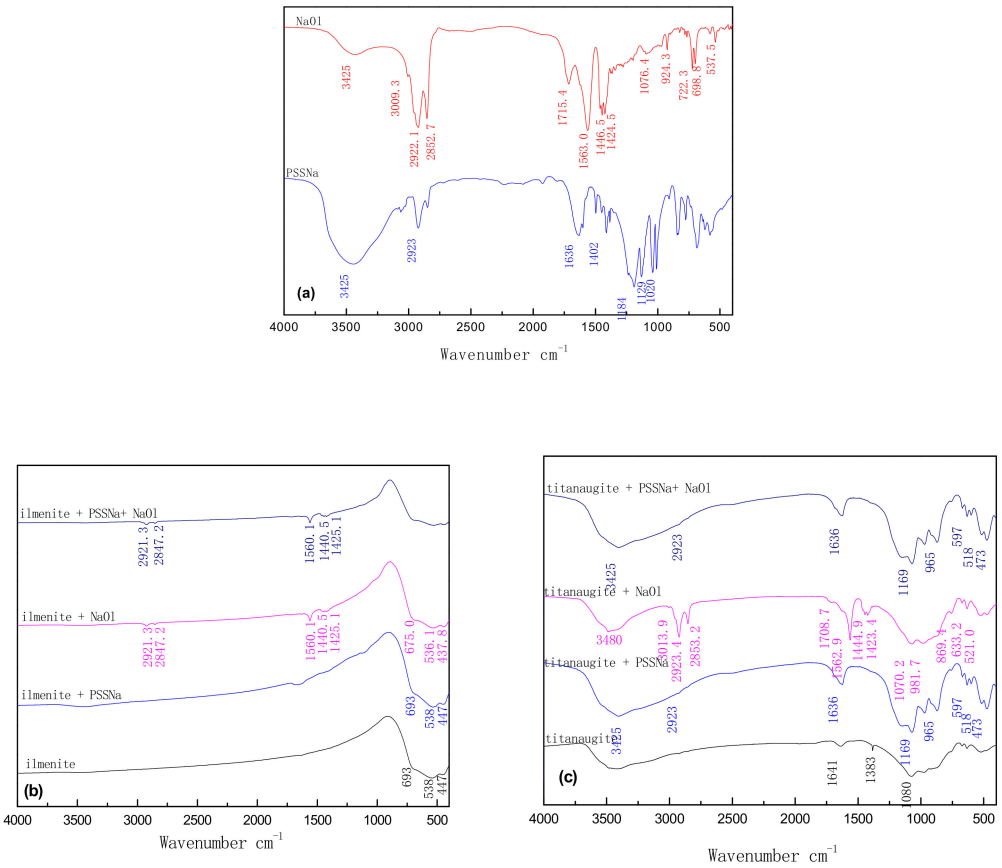

Figure 8. (**a**) Infrared spectra of of PSSNa and NaOl; (**b**) infrared spectra of ilmenite and ilmenite treated with PSSNa, NaOl, PSSNa + NaOl; (**c**) infrared spectra of titanaugite and titanaugite treated with PSSNa, NaOl, PSSNa + NaOl.

3.5. XPS Detection

After the interaction between titanaugite and PSSNa, the XPS full spectrum analysis (a,b) and XPS spectra of various elements on titanaugite (c–f) and titanaugite and ilmenite surface (g,h) were drawn (Figure 9). From the XPS full spectrum analysis of titanaugite and ilmenite treated and not treated with PSSNa, the S characteristic peak was found on the titanaugite surface after treatment with PSSNa, while it did not occur on the ilmenite surface treated with PSSNa, which shows the considerable adsorption of S-containing PSSNa on titanaugite and almost no adsorption of PSSNa on ilmenite. XPS spectra of Ca, Mg, Fe, and Al of titanaugite and Ti and Fe of ilmenite before and after treatment with PSSNa are shown in Figure 9c–h, and the corresponding binding energy and binding energy shifts are listed in Table 4. As displayed in the table, the 0.3 eV shift of $Fe_{2p3/2}$ for ilmenite is larger than the instrumental error of 0.2 eV, which shows that the active sites on the ilmenite surface for PSSNa adsorption are Fe atoms. For titanaugite, the chemical shifts of Ca (1.1 eV), Mg (0.5 eV), Al (0.3 eV), and Fe (0.3 eV) are all greater than 0.2 eV, illustrating that the interactions of PSSNa with the four atoms [32,33].

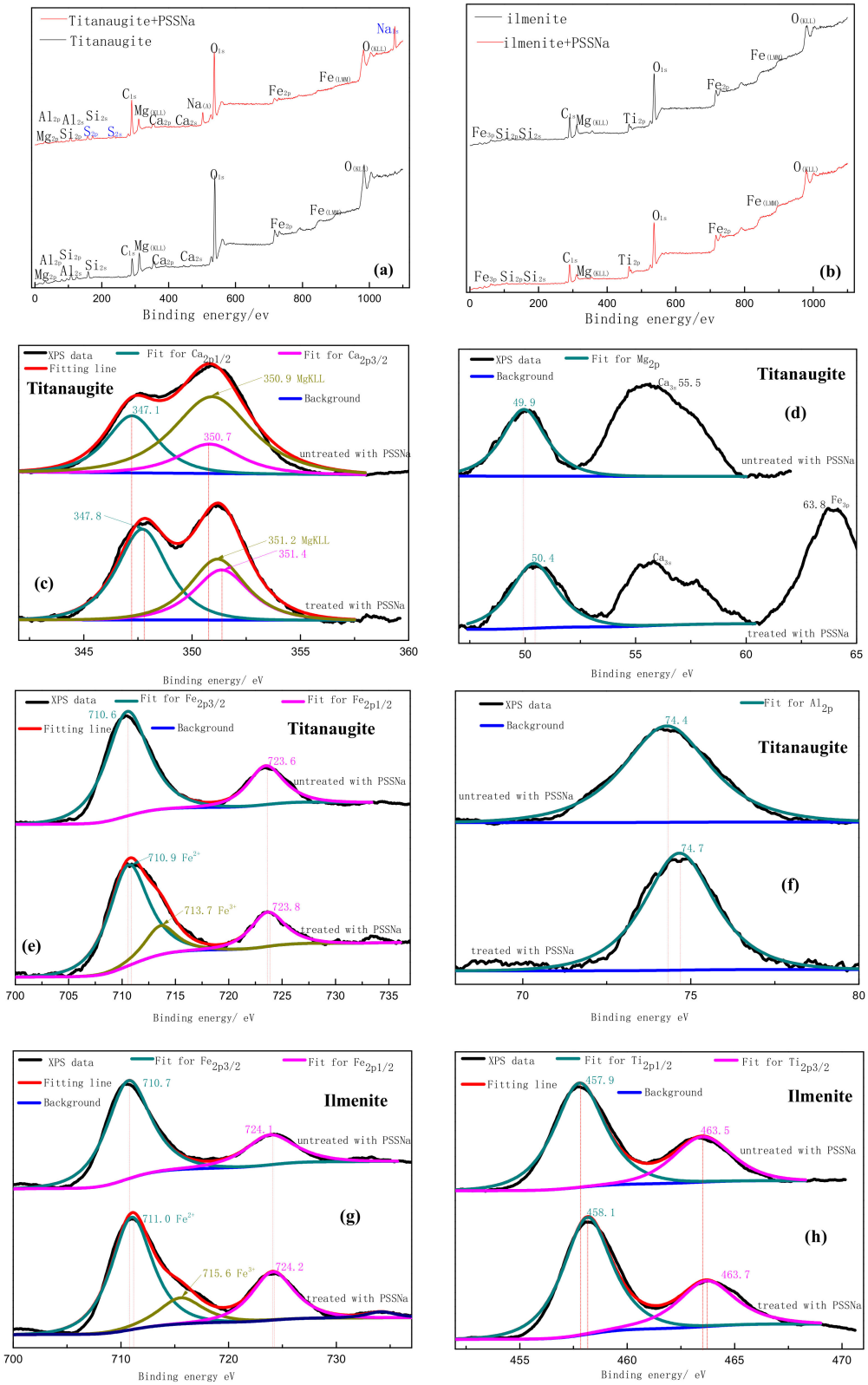

Figure 9. (**a**) XPS spectra of titanaugite surface; (**b**) XPS spectra of ilmenite surface; (**c**–**f**) XPS spectra of Ca, Mg, Fe, and Al on titanaugite surface, respectively; (**g**–**h**) XPS spectra of Fe and Ti on ilmenite surface, respectively.

Table 4. Binding energy valence electrons on titanaugite and ilmenite surfaces.

Minerals	Element	Binding Energy/eV		Chemical Shift ΔE/eV
		Without PSSNa	Treated with Pssna	
Ilmenite	$Fe_{2p3/2}$	710.7	711.0	0.3
	$Fe_{2p1/2}$	724.1	724.2	0.1
	$Ti_{2p3/2}$	463.5	463.7	0.2
	$Ti_{2p1/2}$	457.9	458.1	0.2
Titanaugite	$Ca_{2p3/2}$	347.1	347.8	0.7
	$Ca_{2p1/2}$	350.7	351.4	0.7
	Mg_{2p}	49.9	50.4	0.5
	Al_{2p}	74.4	74.7	0.3
	$Fe_{2p3/2}$	710.6	710.9	0.3
	$Fe_{2p1/2}$	723.6	723.8	0.2

3.6. Suggested Adsorption Model

The interaction model between PSSNa and titanaugite surface is shown in Figure 10. With no PSSNa depressant, NaOl adsorbs on titanaugite through chemisorption according to the interaction of active sites Mg, Ca, Al, and Fe on titanaugite and PSSNa, thus causing the hydrophobicity and flotation of titanaugite. When PSSNa was added before the addition of NaOl, PSSNa adsorbed onto the Ca, Mg, Al, and Fe atoms of the titanaugite surface through parts of the sulfo groups, with other sulfo groups orienting to solution, thus causing the hydrophilicity of the titanaugite surface. Both the steric protection of macromolecular chains and the electrostatic repulsion between the sulfo groups and the negatively charged oleate ions would prevent NaOl from interacting with the titanaugite surface, and thus, the floatability of titanaugite was depressed.

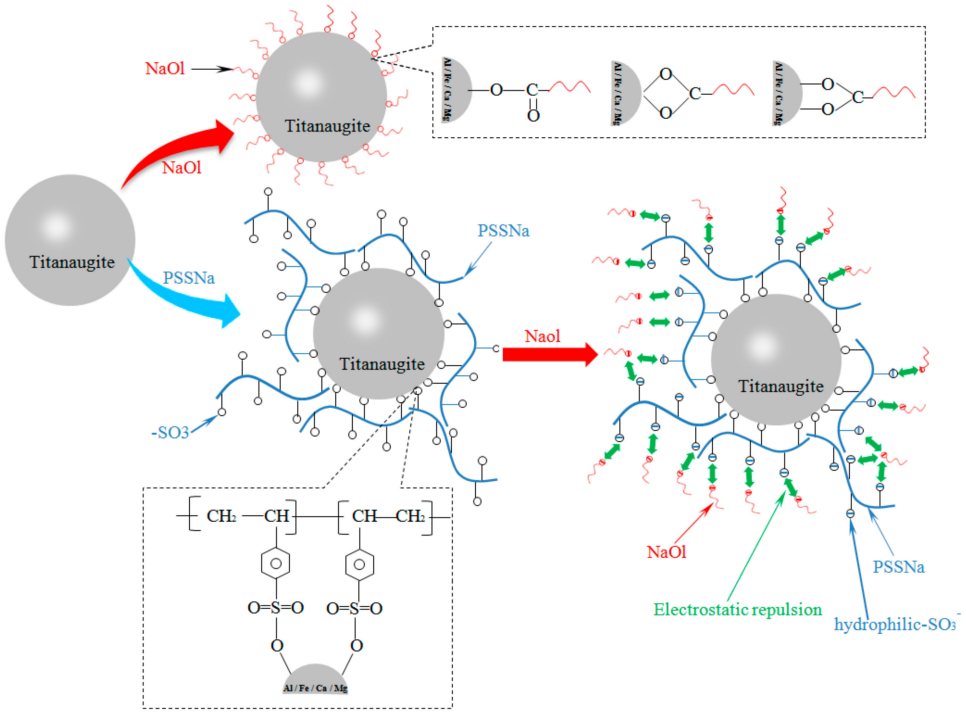

Figure 10. Model schematic diagram of the interaction between titanaugite and PSSNa.

4. Conclusions

(1) The results of flotation for single minerals revealed that PSSNa can expand the gap for recovering titanaugite and ilmenite, and the PSSNa is a selective depressant while separating ilmenite from titanaugite via flotation.

(2) The main gangue associated with actual raw ore (TiO_2 grade: 15.63%) in Panzhihua is titanaugite, and the results of contrast flotation experimentation show that PSSNa is a better depressant than sodium silicate. In a flotation closed circuit test, ilmenite concentrate was obtained with the TiO_2 grade of 45.97% and TiO_2 recovery of 76.32%.

(3) Adsorption quantity test results show that PSSNa can broaden the adsorption quantity gap of NaOl on ilmenite and titanaugite surfaces. The results of adsorption quantity testing are consistent with those of single mineral flotation testing. FTIR testing indicates more obvious chemical adsorption between SO_3^- groups of PSSNa molecules and the titanaugite surface, and further XPS test results show that chemical reactions are mainly between PSSNa and Ca, Mg, Al, and Fe on the titanaugite surface. A negatively charged surface layer forms after PSSNa is absorbed onto the titanaugite surface; active surface sites of titanaugite are occupied with PSSNa/PSS^-, preventing the adsorption of NaOl. In addition, the negative surface potential of adsorbed PSS^- on the titanaugite surface repels NaOl molecules; the floatability of titanaugite was suppressed.

Author Contributions: Author contributions are listed below: conceptualization, J.X. and Y.Z.; methodology and validation, Z.W.; investigation, N.L., B.D. and C.C.; resources, H.W.; data curation, Y.Z. and Z.W.; writing—original draft preparation, N.L.; writing—review and editing, Z.W.; supervision, J.X.; project administration, Y.Z. and H.W.; funding acquisition, Y.Z.

Funding: The authors acknowledge the support of the open fund of the State Key Laboratory of Vanadium and Titanium Resources Comprehensive Utilization, the Geological Environment Survey of Mines in Mining City Panzhihua of China (No. DD20189501), the Sichuan Science and Technology Program of China (No. 2018SZ0282, 2018FZ0092), the National Natural Science Foundation of China (No. 51504199), the Key Laboratory of Sichuan Province for Comprehensive Utilization of Vanadium and Titanium Resources Foundation (No. 2018FTSZ35) and China Geological Big Survey (No. DD20190694).

Conflicts of Interest: The authors declare no conflict of interest. The funders had no role in the design, analyses, and interpretation of any data of the study.

References

1. Chen, D.S.; Zhao, L.S.; Tao, Q.I.; Hu, G.; Zhao, H.X.; Jie, L.I.; Wang, L.N. Desilication from titanium–vanadium slag by alkaline leaching. *Trans. Nonferr. Metal. Soc.* **2013**, *23*, 3076–3082. [CrossRef]
2. Samal, S.; Mohapatra, B.K.; Mukherjee, P.S.; Chatterjee, S.K. Integrated XRD, EPMA and XRF study of ilmenite and titania slag used in pigment production. *J. Alloy. Compd.* **2009**, *474*, 484–489. [CrossRef]
3. Drzymala, J.; Luszczkiewicz, A.; Simiczyjew, P. Flotation study on high-hercynite ilmenite ores. *Int. J. Miner. Process.* **1983**, *10*, 289–296. [CrossRef]
4. Fan, X.; Rowson, N.A. The effect of Pb (NO3)2 on ilmenite flotation. *Miner. Eng.* **2000**, *13*, 205–215. [CrossRef]
5. Farjana, S.H.; Huda, N.; Mahmud, M.A.P.; Lang, C. Towards sustainable TiO2 production: An investigation of environmental impacts of ilmenite and rutile processing routes in Australia. *J. Clean. Prod.* **2018**, *196*, 1016–1025. [CrossRef]
6. Zvyagin, B.B.; Drits, V.A. An introduction to rock forming minerals. Vols. IV by WA Deer, RA Howie and J. Zussman. *J. Appl. Crystallogr.* **1970**, *3*, 426–428. [CrossRef]
7. Mehdilo, A.; Irannajad, M.; Rezai, B. Effect of crystal chemistry and surface properties on ilmenite flotation behavior. *Int. J. Miner. Process.* **2015**, *137*, 71–81. [CrossRef]
8. Bulatovic, S.; Wyslouzil, D.M. Process development for treatment of complex perovskite, ilmenite and rutile ores. *Miner. Eng.* **1999**, *12*, 1407–1417. [CrossRef]
9. Song, Q.; Tsai, S.C. Flotation of ilmenite using benzyl arsonic acid and acidified sodium silicate. *Int. J. Miner. Process.* **1989**, *26*, 111–121. [CrossRef]
10. Wang, D.Z.; Hu, Y.H. *Solution Chemistry of Flotation*; Hunan Scientific Press: Changsha, China, 1988; Volume 2, p. 35.
11. Zhu, Y.G.; Zhang, G.F.; Feng, Q.M.; Yan, D.C.; Wang, W.Q. Effect of surface dissolution on flotation separation of fine ilmenite from titanaugite. *Trans. Nonferr. Metal. Soc.* **2011**, *21*, 1149–1154. [CrossRef]

12. Yang, Y.; Xu, L.; Jia, T.; Liu, Y.; Han, Y. Selective flotation of ilmenite from olivine using the acidified water glass as depressant. *Int. J. Miner. Process.* **2016**, *157*, 73–79. [CrossRef]
13. Liu, X.; Huang, G.Y.; Li, C.X.; Cheng, R.J. Depressive effect of oxalic acid on titanaugite during ilmenite flotation. *Miner. Eng.* **2015**, *79*, 62–67. [CrossRef]
14. Wang, Z.; Xu, L.; Liu, R.; Sun, W.; Xiao, J. Comparative studies of flotation and adsorption with cetyl pyridinium chloride on molybdite and fluorapatite. *Int. J. Miner. Process.* **2015**, *143*, 112–116. [CrossRef]
15. Xiong, F.; Chen, C.; Liu, S. Preparation of chitosan/polystyrene sulfonate multilayered composite metal nanoparticles and its application. *J. Nanosci. Nanotechnol.* **2016**, *16*, 6027–6031. [CrossRef] [PubMed]
16. Wang, Z.; Xu, l.; Wang, J.; Wang, L.; Xiao, J. A comparison study of adsorption of benzohydroxamic acid and amyl xanthate on smithsonite with dodecylamine as co-collector. *Appl. Surf. Sci.* **2017**, *426*, 1141–1147. [CrossRef]
17. Lyu, F.; Gao, J.; Sun, N.; Liu, R.; Sun, X.; Cao, X.; Wang, L.; Sun, W. Utilisation of propyl gallate as a novel selective collector for diaspore flotation. *Miner. Eng.* **2019**, *131*, 66–72. [CrossRef]
18. Liu, J.; Ejtemaei, M.; Nguyen, A.V.; Wen, S.; Zeng, Y. Surface chemistry of Pb-activated sphalerite. *Miner. Eng.* **2020**, *145*, 10658. [CrossRef]
19. Zhang, G.; Zhu, Y.; Feng, Q.; Lu, Y.; Ou, L. Flotation mechanism of fine ilmenite by sodium oleate. *Chin. J. Nonferr. Metal.* **2009**, *2*, 372–377. (In Chinese)
20. Chen, P.; Zhai, J.; Sun, W.; Hu, Y.; Yin, Z. The activation mechanism of lead ions in the flotation of ilmenite using sodium oleate as a collector. *Miner. Eng.* **2017**, *111*, 100–107. [CrossRef]
21. Da Silva, L.; Paula, M.M.S.; Oenning, L.W.; Benavides, R. Properties of polystyrene/acrylic acid membranes after sulphonation reactions. *J. New Mater. Electrochem. Sys.* **2014**, *17*, 085–090.
22. Kong, H.; Luo, P.; Gao, C.; Yan, D. Polyelectrolyte-functionalized multiwalled carbon nanotubes: Preparation, characterization and layer-by-layer self-assembly. *Polymer* **2005**, *46*, 2472–2485. [CrossRef]
23. Nasef, M.M.; Saidi, H.; Dahlan, K.Z.M. Kinetic investigations of graft copolymerization of sodium styrene sulfonate onto electron beam irradiated poly (vinylidene fluoride) films. *Radiat. Phys. Chem.* **2011**, *80*, 66–75. [CrossRef]
24. Cepeda-Jiménez, C.M.; Pastor-Blas, M.M.; Ferrándiz-Gómez, T.P.; MartíN-MartíNez, J.M. Influence of the styrene content of thermoplastic styrene–butadiene rubbers in the effectiveness of the treatment with sulfuric acid. *Int. J. Adhes. Adhes.* **2001**, *21*, 161–172. [CrossRef]
25. Li, H.M.; Liu, J.C.; Zhu, F.M.; Lin, S.A. Synthesis and physical properties of sulfonated syndiotactic polystyrene ionomers. *Polym. Int.* **2001**, *50*, 421–428. [CrossRef]
26. Brijmohan, S.B.; Swier, S.; Weiss, R.A.; Shaw, M.T. Synthesis and characterization of cross-linked sulfonated polystyrene nanoparticles. *Ind. Eng. Chem. Res.* **2005**, *44*, 8039–8045. [CrossRef]
27. Xing, W.; Ma, Q.; Xu, J.; Peng, X. Baeyer–Villiger oxidation of cyclic ketones with hydrogen peroxide catalyzed by silica–VTMO–OSO3H. *J. Porous Mater.* **2015**, *22*, 487–492. [CrossRef]
28. Wang, L.; Sun, N.; Wang, Z.; Han, H.; Yang, Y.; Hu, Y.; Tang, H.; Liu, R. Self-assembly of mixed dodecylamine–dodecanol molecules at the air/water interface based on large-scale molecular dynamics. *J. Mol. Liq.* **2019**, *276*, 867–874. [CrossRef]
29. Bekri-Abbes, I.; Bayoudh, S.; Baklouti, M. Converting waste polystyrene into adsorbent: Potential use in the removal of lead and cadmium ions from aqueous solution. *J. Polym. Environ.* **2006**, *14*, 249–256. [CrossRef]
30. Cruz-Cruz, I.; Reyes-Reyes, M.; López-Sandoval, R. Formation of polystyrene sulfonic acid surface structures on poly (3, 4-ethylenedioxythiophene): Poly (styrenesulfonate) thin films and the enhancement of its conductivity by using sulfuric acid. *Thin Solid Films* **2013**, *531*, 385–390. [CrossRef]
31. Wang, Z.; Wang, L.; Wang, J.; Xiao, J.; Liu, J.; Xu, L.; Fu, K. Strengthened floatation of molybdite using oleate with suitable co-collector. *Miner. Eng.* **2018**, *122*, 99–105. [CrossRef]
32. Wang, Z.; Wang, L.; Zheng, Y.; Xiao, J. Role of calcium dioleate in the flotation of powellite particles using oleate. *Miner. Eng.* **2019**, *138*, 95–100. [CrossRef]
33. Xiao, J.; Zhang, Y. Recovering Cobalt and Sulfur in Low Grade Cobalt-Bearing V–Ti Magnetite Tailings Using Flotation Process. *Processes* **2019**, *7*, 536. [CrossRef]